

1 Mathematical formulation

2D isentropic vortex flow was studied by Yee, Vinokur and Djomehri (1999) and Shu (1998). We start with uniform base flow and superimpose perturbation to get an isentropic vortex. The result of this initialization is a pure advection of the vortex at the base flow velocity. The base flow is

$$\rho_b = 1.0, \quad (1)$$

$$u_b = u_\infty, \quad (2)$$

$$v_b = v_\infty, \quad (3)$$

$$p_b = \rho_b^\gamma, \quad (4)$$

$$T_b = T_\infty. \quad (5)$$

The perturbations are

$$\delta u = -\beta \exp(1-r^2) \frac{(y-y_o)}{2\pi}, \quad (6)$$

$$\delta v = \beta \exp(1-r^2) \frac{(x-x_o)}{2\pi}, \quad (7)$$

$$\delta T = -\left(\frac{(\gamma-1)\beta^2}{16\gamma\pi^2}\right) \exp[2(1-r^2)]. \quad (8)$$

Where $r = \sqrt{(x-x_o)^2 + (y-y_o)^2}$ and the center of the vortex is at (x_o, y_o) . With this we can initialize the flow by using the following relations

$$u = u_b - \beta \exp(1-r^2) \frac{(y-y_o)}{2\pi}, \quad (9)$$

$$v = v_b + \beta \exp(1-r^2) \frac{(x-x_o)}{2\pi}, \quad (10)$$

$$T = T_b - \left(\frac{(\gamma-1)\beta^2}{16\gamma\pi^2}\right) \exp[2(1-r^2)] \quad (11)$$

$$\rho = T^{1/(\gamma-1)}, \quad (12)$$

$$p = \rho^\gamma, \quad (13)$$

$$\rho e = \frac{p}{\gamma-1} + \frac{\rho}{2}(\mathbf{u}^2). \quad (14)$$

2 Test cases

Following table list all the test cases that we have performed. In all of these cases the domain size was $x = [0, 10]$ and $y = [-5, 5]$. Apart from the long run case, all other cases are run for $t = 10$ i.e. the vortex passes through the downstream periodic boundary once and comes back to its initial position. Pseudo-color plots of conserved variables at initialization are shown in 1. The exact solution of this problem advects this initial condition as per the base flow. In all our cases base flow velocity is unity and it is x direction (except for flip direction case, see Table 1). We typically run the case for 10 time units so that the vortex comes back to its initial position. L2 norms of the error in the 5 conserved variables are computed as the flow evolves.

Figure 3 compares all the 5 conserved variables after the simulation has completed time integrating the governing equations to $t = 10$ for the coarsest and finest grids. In both cases the vortex is advected at the correct speed. However, the coarse grid resolution is too coarse to resolve and maintain the shape of the vortex.

We have carried out p-refinement and h-refinement to study the convergence of CMT-Nek. Lets consider the p-refinement cases. We have 3 domain decompositions giving rise to 25 (5x5), 100(10x10) and 400(20x20) elements. In each case, we increase the polynomial order from 5 to 15 and run the simulation for $t=10$ time units. L2 norms of the error in all 5 conserved variables at $t=10$ are plotted to determine the convergence rate. The convergence plots are shown in figure 4. These plots prove that CMT-Nek gives exponential convergence (p-refinement) for smooth solutions. Figure 5 shows the convergence plots for h-refinement study. From the figure it is clear that increasing the polynomial order changes the slope of L2 norm. The curve fits shown in the figure are not precise, I played with the power and adjustable constants to obtain a line that passes through the 3 data points.

Table 1: List of simulations. * Curved faces runs use 4x4 and 8x8 elements. Both 4x4 and 8x8 elements uses 5,10,15,20 and 25 polynomial orders.

case	20x20	10x10	5x5
Nxd=2*Nx1	5, 6, 7, 8, 9, 10, 15	5, 6, 7, 8, 9, 10, 15	5, 6, 7, 8, 9, 10, 15
Long run $t = 50$	-	10	-
Curved faces*	-	-	-
Change flow direction	-	-	5, 10, 15

3 Curved element faces

Next task in this study to evaluate the effect of curved grids on the convergence rate. NEK reads the grid from the input file (`{casename}.REA`). NEK allows users to modify the grid read from the input file as a part of the initialization process. NEK ensures that

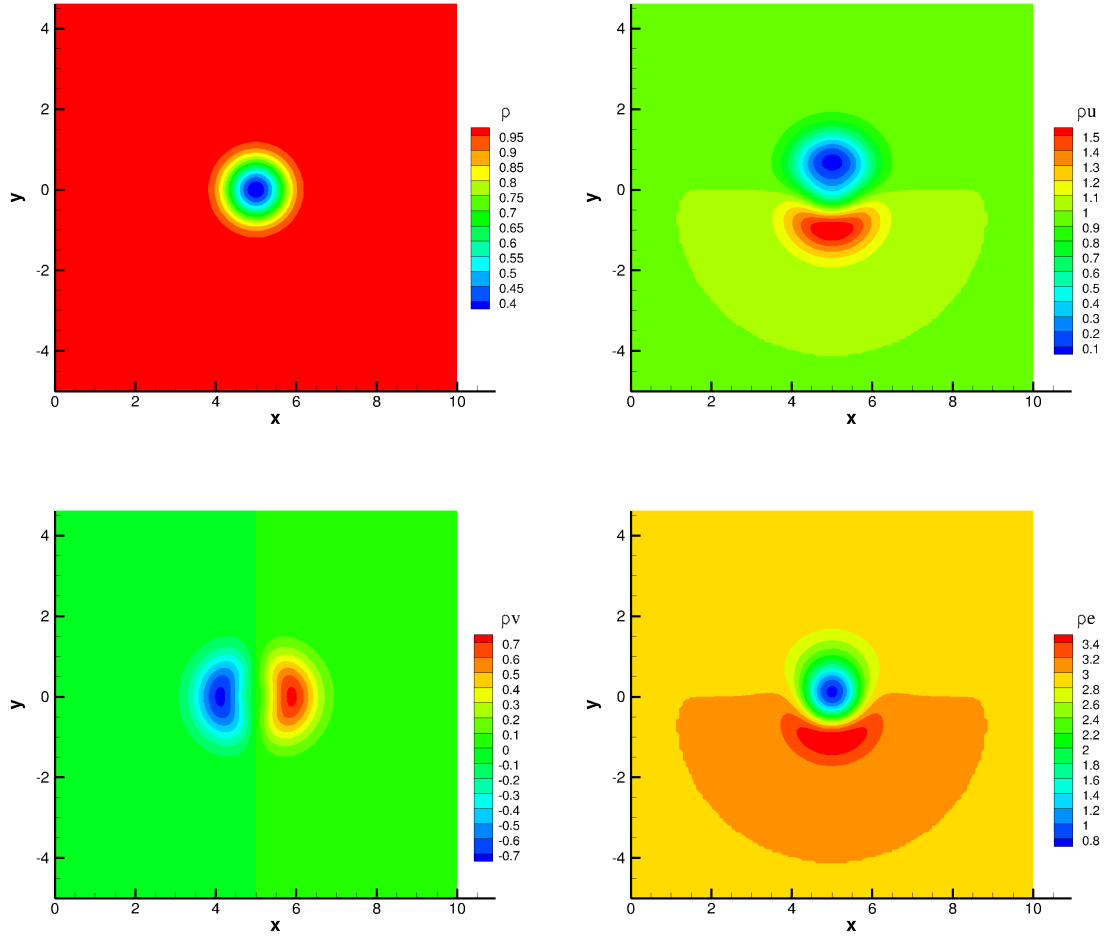


Figure 1: Pseudo-color plots of 5 conserved variables at initialization.

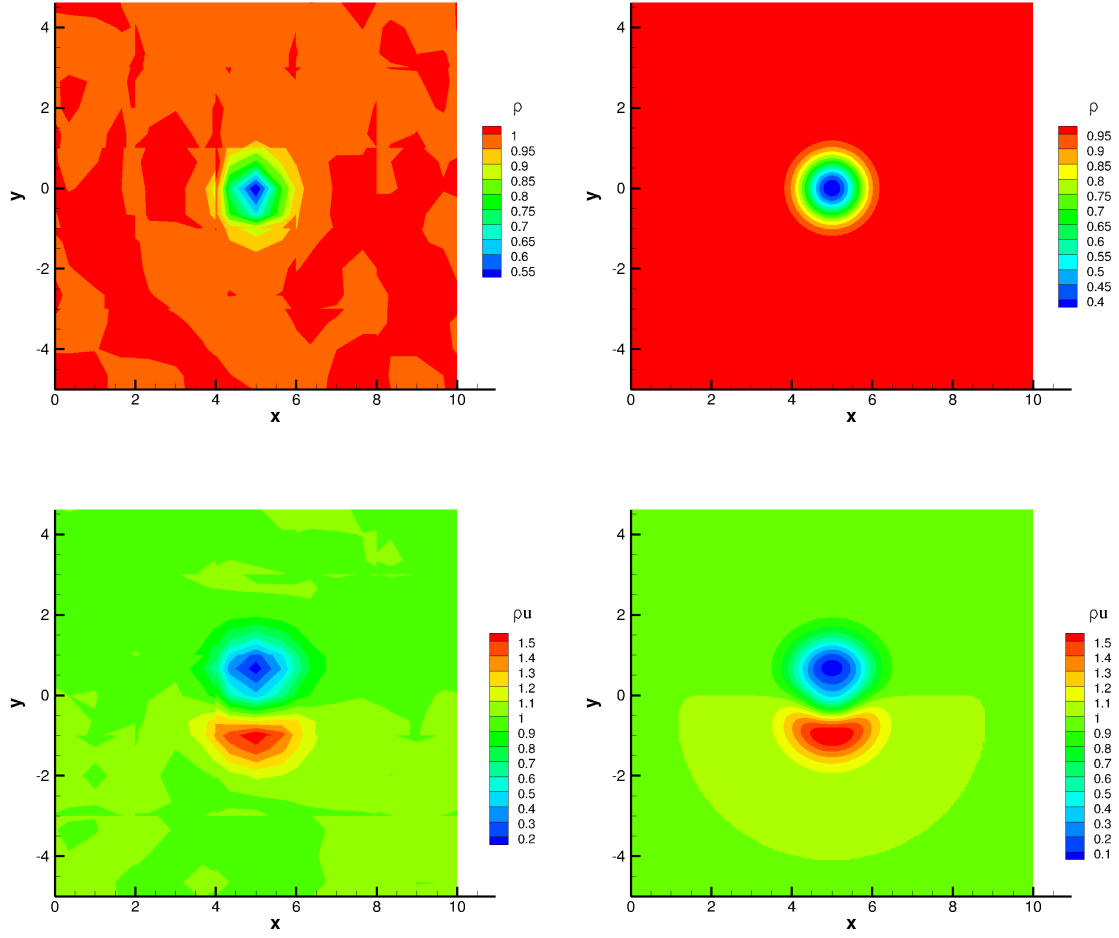


Figure 2: Pseudo-color plots of ρ and ρu for coarsest and finest resolutions. Coarsest resolution is 25 element case with $N=5$ and the finest resolution is 400 element case with $N=15$.

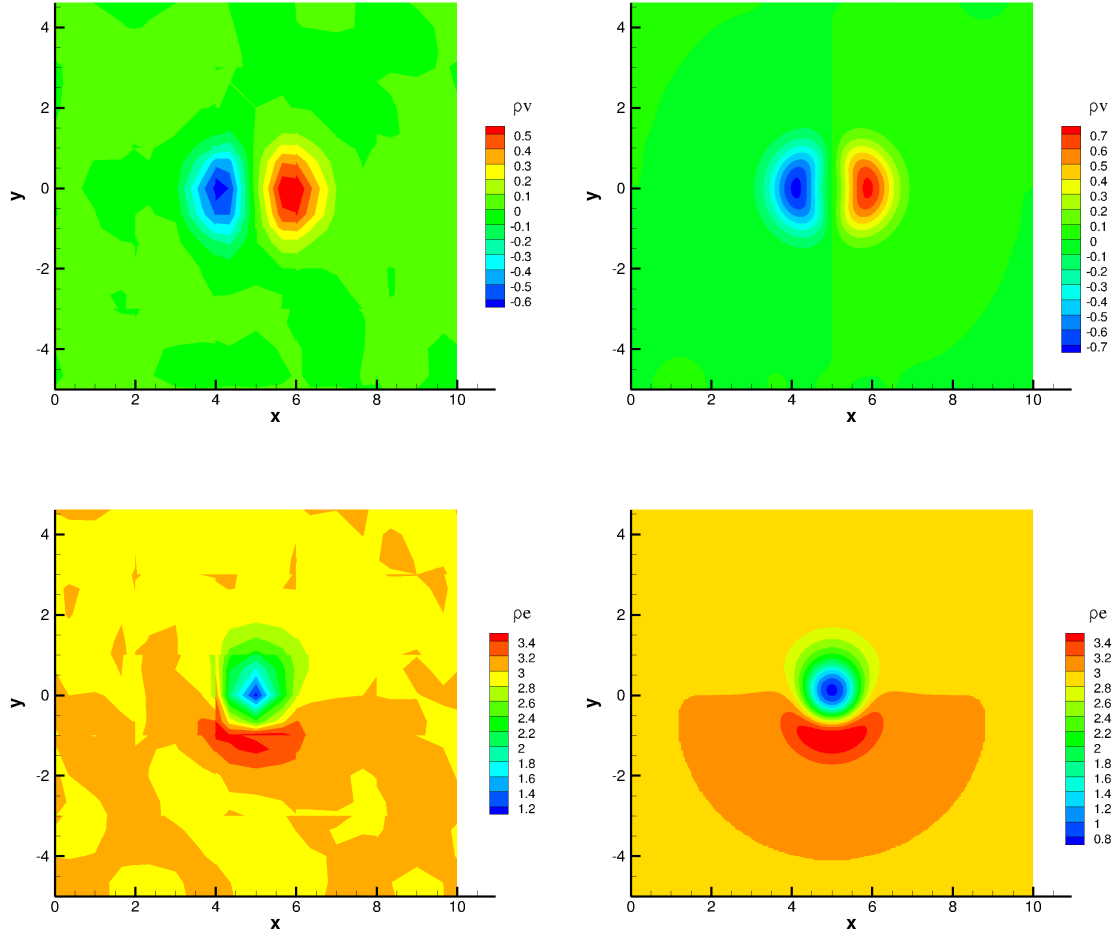


Figure 3: Pseudo-color plots of ρv and ρe for coarsest and finest resolutions. Coarsest resolution is 25 element case with $N=5$ and the finest resolution is 400 element case with $N=15$.

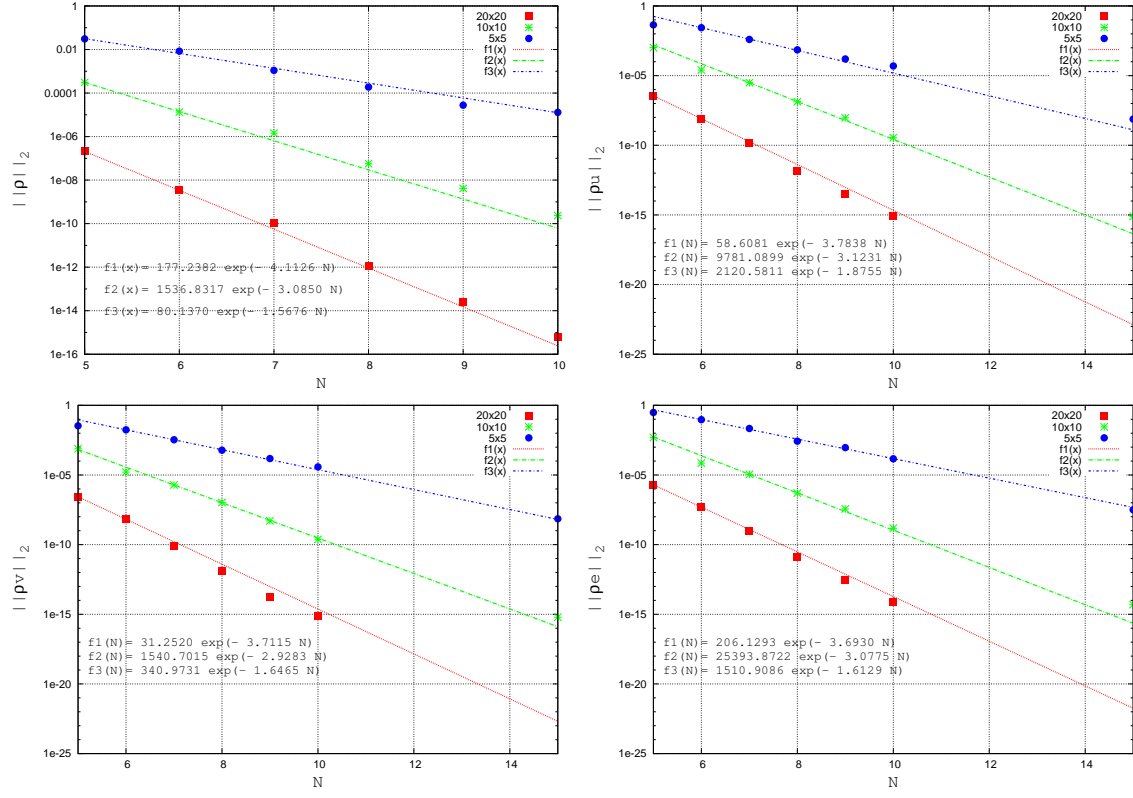


Figure 4: Convergence plots of 5 conserved variables for p-refinement.

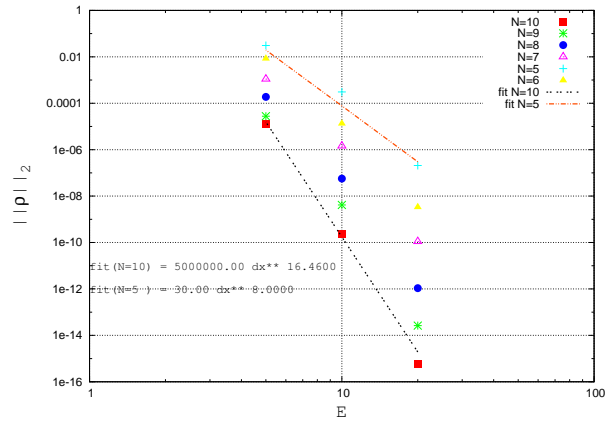


Figure 5: Convergence plot of L2 norm of error in ρ for h-refinement.

the modifications made to the grid result in re-evaluating the metrics and mapping to the reference element. Another way of incorporating curved elements is using PREX utility which is a GUI for generating input file (`jcasename.j.REA`) for NEK.

Here we have used both options to generate curved elements. The former option is simple but the deformations to the cartesian grid have to be a function of the polynomial order in the element so that the location of GLL points consistently lie within its boundaries. Interpreting results when the shape of the elements is integrally coupled to the polynomial order is difficult. Hence we choose to generate curved elements using the PREX utility. This section briefly summarizes the results.

In order to systematically study the effect of curved interfaces on the convergence results, we considered 4 types of deformations.

1. Straight element faces, but the vertices are displaced such that the elements are no longer squares. See figure 6
2. Element vertices are left unchanged but the faces are now arcs of a circle. See figure 6.
3. Element vertices are displaced and the faces are arcs of a circle. See figure 6.
4. All of the above modification are done to a 4x4 element decomposition of a 10x10 box. Here we refine the 10x10 box to be decomposed into 8x8 elements and the element faces are made arcs of a circle. See figure 6

In all these cases we recover exponential convergence as the polynomial approximation inside the element is increased. Convergence results are shown in figure 7. The first subplot compares the p-refinement results for 4 grids starting from the regular cartesian grid to the most deformed grid, i.e. grid where the vertices are moved and the faces are made arc of a circle. Observe that L2 error norms for a given polynomial approximation increases as the grids are deformed more. Nevertheless the exponential convergence on p-refinement is maintained. Note that the exponential convergence factor drops as the grids are deformed more. We expect this behavior as some of the DOFs are used to resolved/approximate the deformed geometry. In the second subplot, we compare the convergence results for 4x4 and 8x8 grid. Even here the exponential convergence is recovered.

4 Change of flow direction

Another useful test is to change the flow direction and re-run some of the cases to ensure that CMT-Nek convergence results are independent of flow direction. This also helps us catch any systematic bugs in the code. Figure 8 shows the p-refinement convergence for 3 polynomial orders used in a 5x5 element decomposition of a 10x10 box. The convergence results are compared with its corresponding case where the flow was in x direction. It is evident from the plot that we recover exponential convergence, and the L2 error norms for

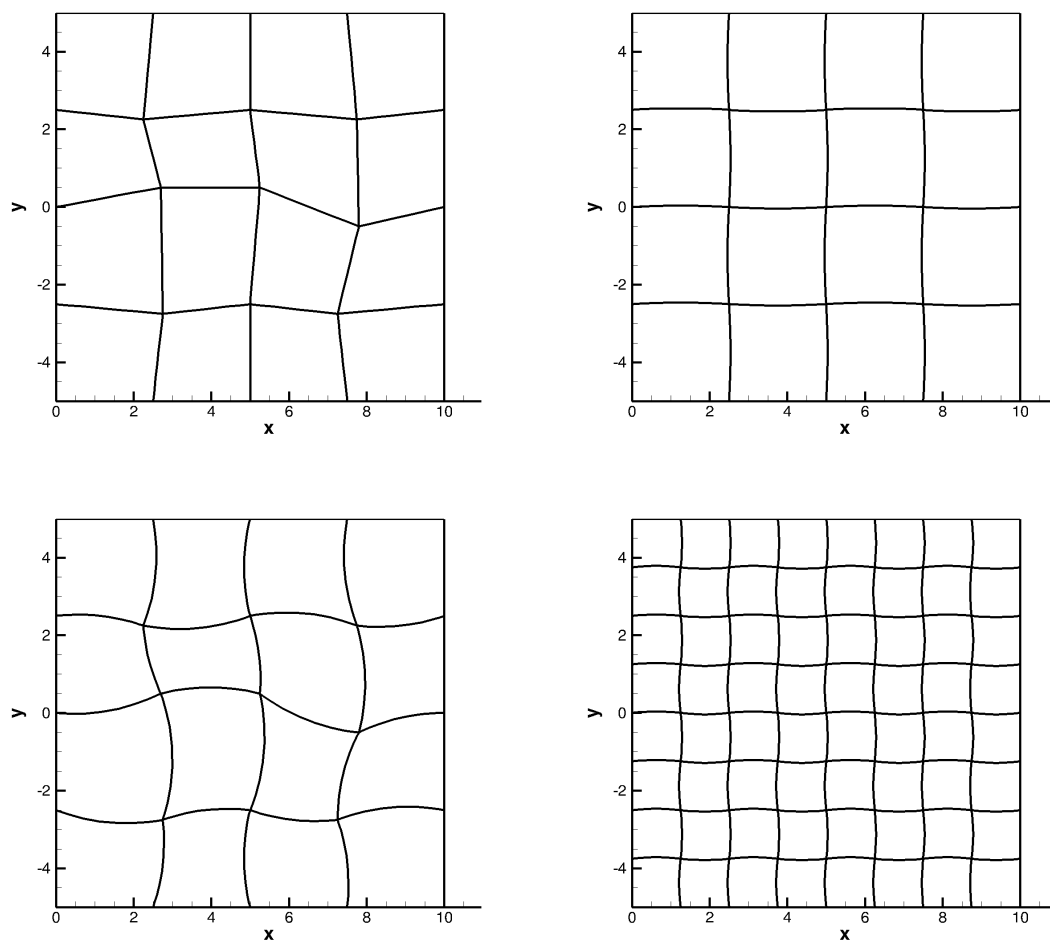


Figure 6: Curved grids used in the p-refinement convergence study.

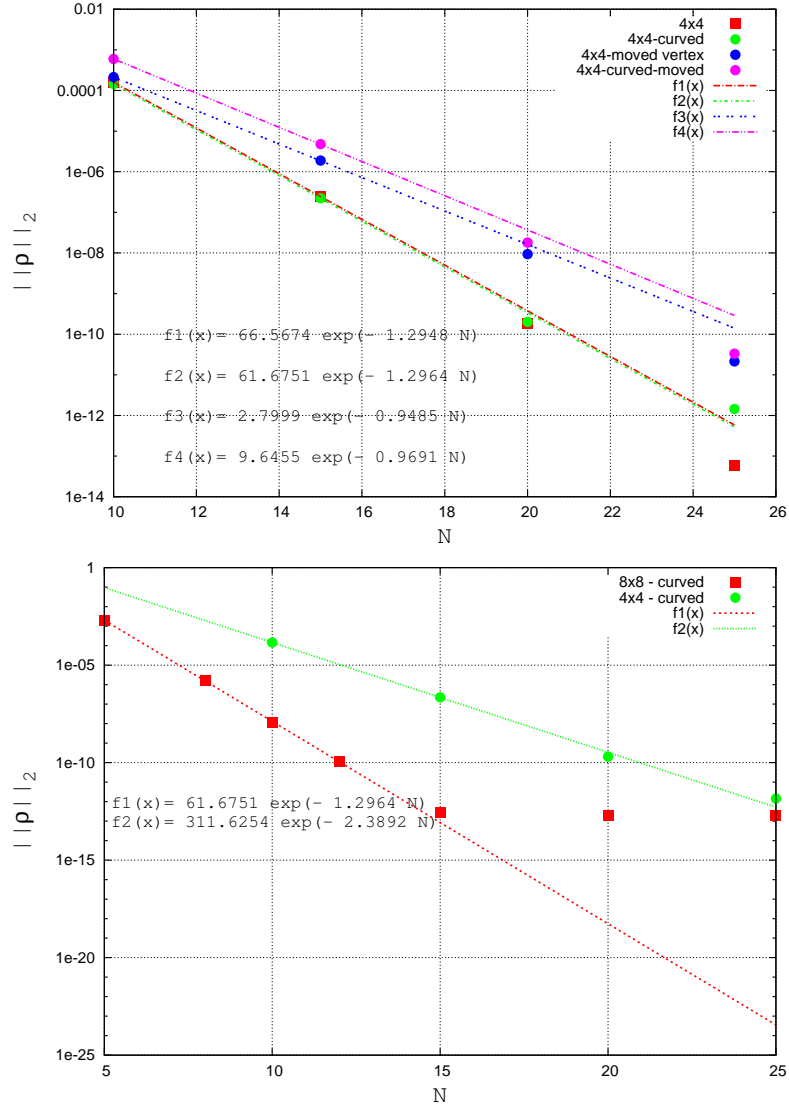


Figure 7: Convergence plots for p-refinement on various curved grids.

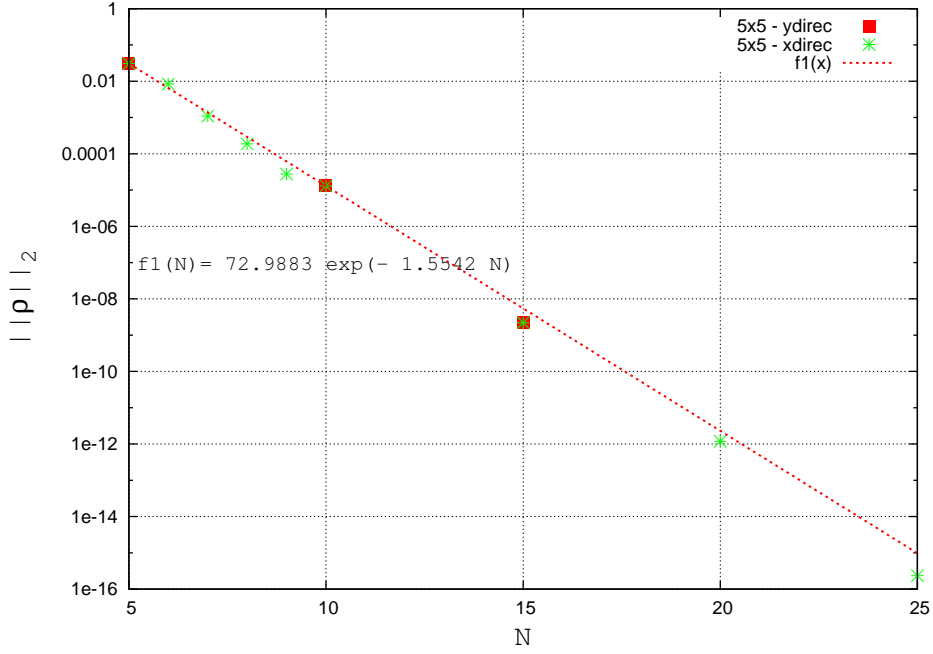


Figure 8: Convergence plots for p-refinement on various curved grids.

the 3 polynomial orders are right on top of the corresponding cases when the flow was in x direction.

5 Long run results

We have also ran one case (see table 1) for long time so that the vortex passes over its initial location 5 times. The objective of this run was to ensure the stability of CMT-Nek and observed the evolution of L2 error norms over time. Figure 9 shows the pseudo color plots of the conserved variables after the vortex has been advected 5 times over the streetwise periodic boundary. Figure ?? shows the time evolution of L2 error norms. We do not see saturation in the L2 error norm in time. This issue may need further investigation.

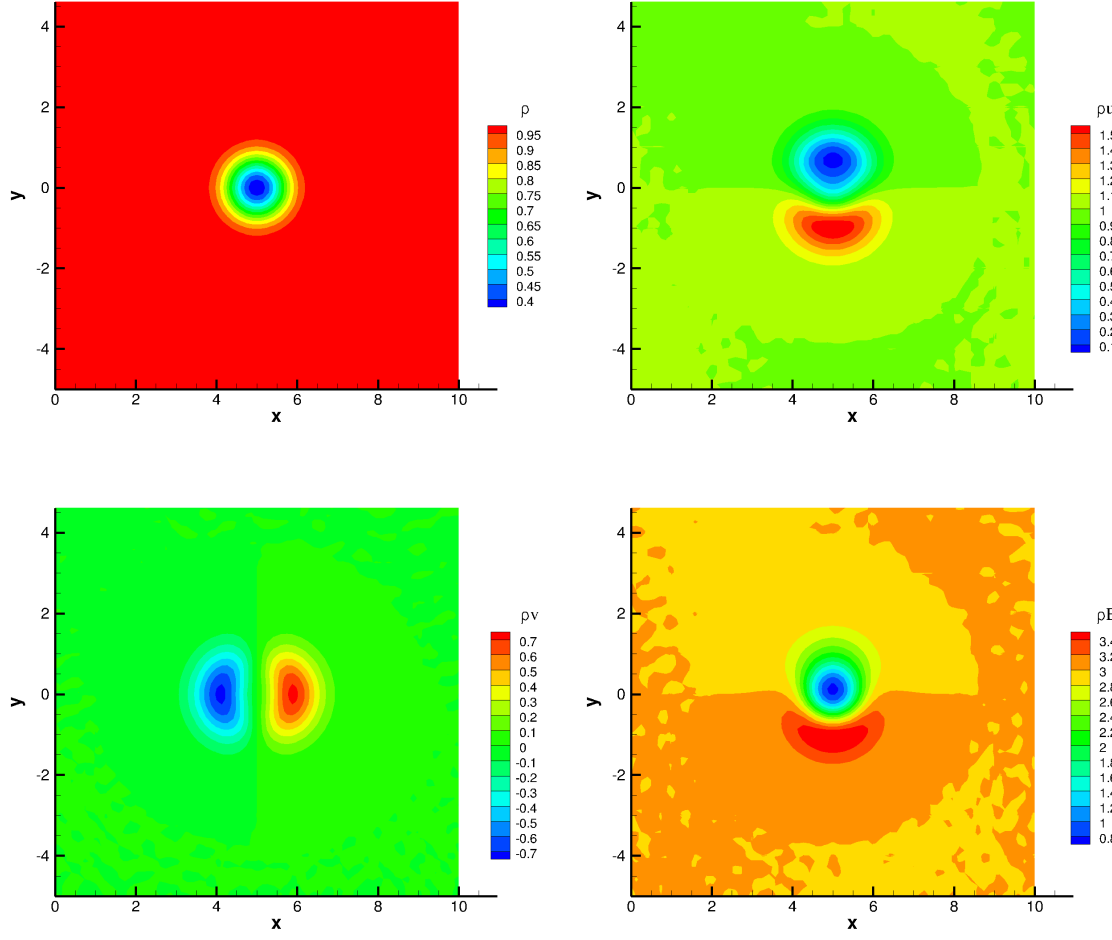


Figure 9: Pseudo-color plots of ρ , ρu , ρv and ρE for 10x10 elements with $N=10$. These plots are after $t = 50$, i.e. the vortex has been advected through the periodic streetwise boundary 5 times.

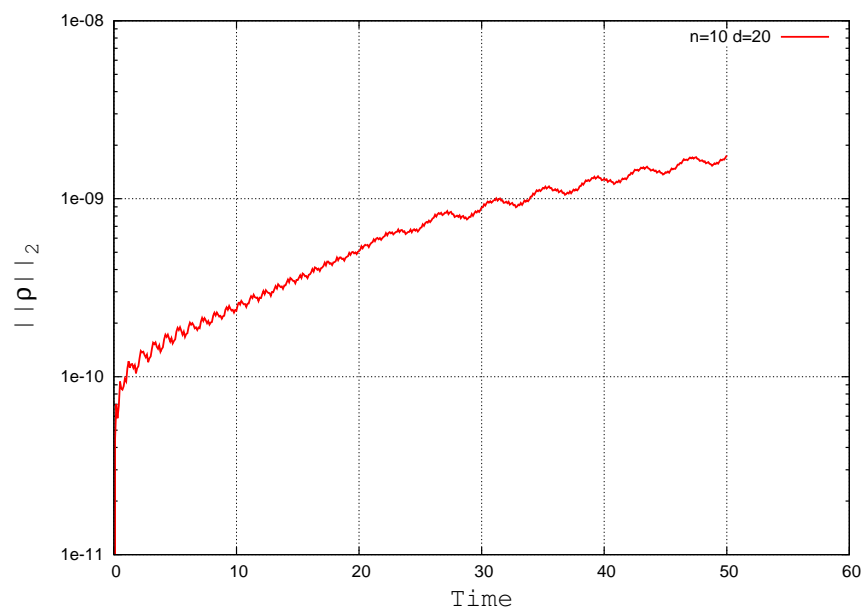


Figure 10: Time evolution of L2 error norm.